From spectral analysis to hysteresis loops: A breakthrough in the optimization of magnetic nanomaterials for bioapplications

JPhys Materials

PURPOSE-LED PUBLISHING™

PAPER • OPEN ACCESS

From spectral analysis to hysteresis loops: a breakthrough in the optimization of magnetic nanomaterials for bioapplications

To cite this article: Gabriele Barrera *et al* 2023 *J. Phys. Mater.* **6** 035007

Journal of Physics: Materials

PAPER

From spectral analysis to hysteresis loops: a breakthrough in the optimization of magnetic nanomaterials for bioapplications

Gabriele Barrera*, Paolo Allia and Paola Tiberto

INRiM, Advanced Materials Metrology and Life Sciences, Torino I-10135, Italy
* Author to whom any correspondence should be addressed.

E-mail: g.barrera@inrim.it

Keywords: magnetic nanomaterials, magnetic nanoparticles, hysteresis loops, magnetic frequency analysis

Supplementary material for this article is available online

OPEN ACCESS

RECEIVED
13 January 2023

REVISED
3 May 2023

ACCEPTED FOR PUBLICATION
2 June 2023

PUBLISHED
13 June 2023

Abstract

An innovative method is proposed to determine the most important magnetic properties of bioapplication-oriented magnetic nanomaterials exploiting the connection between hysteresis loop and frequency spectrum of magnetization. Owing to conceptual and practical simplicity, the method may result in a substantial advance in the optimization of magnetic nanomaterials for use in precision medicine. The techniques of frequency analysis of the magnetization currently applied to nanomaterials both *in vitro* and *in vivo* usually give a limited, qualitative picture of the effects of the active biological environment, and have to be complemented by direct measurement of the hysteresis loop. We show that the very same techniques can be used to convey all the information needed by present-day biomedical applications without the necessity of doing conventional magnetic measurements in the same experimental conditions. The spectral harmonics obtained analysing the response of a magnetic tracer in frequency, as in magnetic particle spectroscopy/imaging, are demonstrated to lead to a precise reconstruction of the hysteresis loop, whose most important parameters (loop's area, magnetic remanence and coercive field) are directly obtained through transformation formulas based on simple manipulation of the harmonics amplitudes and phases. The validity of the method is experimentally verified on various magnetic nanomaterials for bioapplications submitted to ac magnetic fields of different amplitude, frequency and waveform. In all cases, the experimental data taken in the frequency domain exactly reproduce the magnetic properties obtained from conventional magnetic measurements.

1. Introduction

The last two decades have witnessed a boost of biomedical applications based on the unique properties of magnetic nanomaterials [1–4]. Magnetic single core [5] and multi-core nanoparticles [6], either bare [7] or submitted to surface functionalization [8, 9], core–shell systems [10, 11], supraparticles [12], hollow nanoparticles [13], nanochains [14, 15] and nanodiscs [16, 17] are being actively investigated in view of their application in modern therapies of precision medicine [18, 19] as well as in radiation-free, non-invasive imaging or spectroscopy techniques and in the development of sensitive bionsensors [20–22]. A common feature of most of the above mentioned applications is that they typically make use of magnetic nanomaterials driven at high frequency in the non-linear magnetization regime [23] (the strictly linear magnetization regime, i.e. the ac magnetic susceptibility [24], is nowadays investigated as a function of frequency mainly for characterization purposes). The interest towards magnetic nanomaterials is enhanced by their multifunctional features, such as the capacity to act as point-like sensing elements in magnetic particle imaging (MPI) and spectroscopy (MPS) [25], point-like heat generators in magnetic particle hyperthermia [26], magnetically driven nanocarriers for drug delivery [27].

The functional properties of magnetic nanomaterials arise from the rotation (or switch) of the magnetization vector by effect of an ac field $H(t)$. In magnetic hyperthermia, it is the behaviour of the

magnetization M with the driving field H which gives rise to the predominant heating effect [26, 28], so that the research focus is on the properties of the $M(H)$ curve which results by plotting the magnetization $M(t)$ as a function of the driving field $H(t)$.

On the other hand, important applications such as MPI, MPS and biosensors are based on the analysis of the magnetization process in the frequency domain rather than in the time domain, and make use of the spectral amplitudes of the periodic magnetization (or the corresponding voltage induced in a pickup coil) excited either by applying a single-frequency driving field or by exploiting suitable frequency-mixing techniques [21, 22]. In applications involving spectral analysis of the magnetic signal, exactly determining the actual dependence of M on the driving field seems to be of lesser importance; however, an imperfect knowledge of the behaviour of M with H can lead to negative consequences. An example of the drawbacks of an ill-defined magnetization curve in the MPI image reconstruction has been recently discussed [29].

As a matter of fact, the magnetization process of a nanomaterial is sensitive to the environment where it is placed, being influenced by the physical nature of the host medium (e.g. whether it is a solid or a viscous fluid) [30] and by the chemical features of the surrounding species able to interact with its surface [31]. In particular, the $M(H)$ curve can be modified by a variety of physicochemical effects or transformations on the nanometer scale, such as growth or accretion of single particles, clustering, aggregation, selective linking to non-magnetic species [32–35]. Analysing the changes of the $M(H)$ curve provides a key to monitor these effects in real time.

The interpretation of the magnetic behaviour of nanomaterials is often hindered by the intrinsic complexity of the magnetization process, which usually displays hysteretic features. Magnetic hysteresis, originated by the intrinsic irreversibility of the magnetization rotation or switch [36], is not to be neglected when a magnetic nanomaterial is used either as a heat generator [28, 37] or as a contrast agent [38]. It should be recognized that hysteresis of the magnetization is the rule rather than the exception in nanomaterials for application in biomedicine, which are typically submitted to high-frequency fields so that frequency-sustained hysteresis [39, 40] often appears. This happens even in nanomaterials exhibiting a genuine superparamagnetic behaviour in dc measurements, such as the SPION (superparamagnetic iron oxide nanoparticles) [41]. Although magnetic hysteresis is a complex phenomenon [36], it is not *per se* a detrimental effect for the current bioapplications of magnetic nanomaterials; quite on the contrary, it can be exploited to improve their performance [28]. In spite of the inherent difficulty of interpretation, hysteresis loop measurements help to draw a picture of the physicochemical processes occurring on the nanometer scale in an active environment.

Spectral analysis too provides some information about the environment of magnetic nanoparticles, because the amplitude of the higher-order harmonics of the line spectrum of the picked up signal is sensitive to the physical state of the host material [42–45] and therefore to the effects of the hosting tissue on tracer mobility [21, 46]; however, directly relating a change of the spectral harmonics to a specific effect taking place in the environment can be hard to do.

Such a difficulty could be overcome (or at least attenuated) by routinely associating to spectral analysis the knowledge of the magnetization curve $M(H)$ in the same operating conditions. However, combining the two pieces of information is not an easy task, because magnetic measurements require measuring techniques and setups which are rather different from the ones typically used in magnetic spectroscopy. Moreover, magnetic measurements are usually difficult to do owing to the weak magnetic signal produced by a sparse assembly of nanomagnets. A few examples of experimental procedures linking the spectral harmonics of $M(t)$ to the hysteresis loops are discussed in the literature. In particular, reconstructing $M(H)$ loops from frequency-domain spectra by means of a numerical Inverse Fast Fourier Transform was proposed in view of ac-field applications of nanoparticles [47, 48]; besides, a method to correct distortions in the $M(t)$ signal by applying a frequency-dependent term to each harmonic of the picked-up voltage was envisaged and successfully exploited [49].

It would be highly desirable to develop a simple mathematical tool to link the spectral harmonics of the periodic magnetization to hysteresis loops, obtaining at the same time the main application-oriented loop parameters without the need of actually doing any additional ad hoc measurement.

We show that a univocal relation between the line spectrum of the periodic magnetization (or the voltage induced in a pickup coil) and the corresponding hysteresis loop in the (H,M) plane is rather easy to derive, because both properties contain the same amount of information about the magnetization process.

In section 3 it is shown how the spectral harmonics of the frequency line spectrum of the signal can be used to reconstruct the magnetization curve in the (H,M) plane. Specific transformation formulas are proposed in section 4 to get important parameters of the hysteresis loop (such as loop's area, magnetic remanence and coercive field) by simple manipulation of the amplitudes and phases of the spectral harmonics.

The ability of the proposed analytical expressions to reconstruct the hysteresis loop from the line spectrum and the adequacy of the transformation formulas are experimentally verified in sections 5 and 6 on some magnetic nanomaterials eligible for bioapplications. These belong in different classes (nanoparticles, powders, nanodiscs) and are submitted to ac magnetic fields of different amplitude, frequency and waveform. Materials and measurement techniques are reviewed in section 2. In all cases, the experimental data taken in the frequency domain are shown to exactly reproduce the magnetic properties obtained from measurements done in the time domain. A similar check is made on a macroscopic magnetic material, an extra-soft amorphous ferromagnetic ribbon of prospective use in sensing devices for biomedical applications based on the giant magnetoimpedance effect [50]. Even in this case the proposed method of conversion is fully satisfactory, showing that the results obtained in this paper have general validity and can be applied in principle to magnetic materials of all types and sizes. Finally, a case study is discussed in some detail in section 6 to elucidate the advantage of combining magnetic measurements in time and frequency domains.

2. Experimental

2.1. Magnetic materials

Magnetite (Fe_3O_4) nanoparticles were prepared by a non-hydrolytic sol-gel (NHSG) process in the presence of benzyl alcohol (BzOH) following the synthesis procedure described elsewhere [51]. The $Fe(AcAc)_3$:BzOH ratio was fixed at 0.03. The resulting Fe_3O_4 NPs are characterized by an average size of about 7 nm with a narrow dispersion ($<$1 nm) around the mean value, and an aspect ratio of 1.13 [51].

$Co_{0.84}Zn_{0.16}Fe_2O_4$ ferrite powders were prepared by a sol-gel auto-combustion method utilizing citrate-nitrate precursors at low temperature ($\leqslant$110 °C) without any post-preparation heat treatments, as described elsewhere [52]. The morphology of the synthesized Co-Zn ferrite is a quite complex grain arrangement consisting in a micrometer-sized agglomerate with surface similar to a beehive composed of nanosized crystals (grains). X-ray diffraction (XRD) reveals a grain mean diameter of 34.9 nm [52].

An amorphous ribbon of composition $Fe_{62.50}$ $Ni_{10.00}$ $Si_{11.05}Cr_{2.23}B_{11.14}C_{3.09}$ was obtained by the melt-spinning technique. The pre-alloy was prepared and then inductively re-melted in a quartz tube with a nozzle (0.8 mm diameter) under vacuum atmosphere, and subsequently injected onto a rotating copper wheel by applying a high-purity Ar pressure. The thickness of the produced ribbons is about 40 μm.

Au-coated permalloy ($Ni_{80}Fe_{20}$) nanodiscs (diameter: 630 nm) were produced by combining polystyrene nanosphere lithography and sputtering [53]. A metallic trilayer comprised of a 30 nm permalloy film sandwiched between two 5 nm Au films was deposited on a Si substrate coated by a resist layer. The Au coatings were deposited with the purpose of making the nanodisc surface biocompatible and apt to be bio-functionalized [53].

By dissolving the sacrificial resist underlayer in acetone, the nanodiscs were detached from the substrate and dissolved in water. The disc were magnetically characterized both before detachment and in water solution.

2.2. Methods

Quasi-static (dc) magnetization curves were measured at room temperature by means of a Lakeshore 7200 vibrating sample magnetometer (VSM) in the magnetic field range $\pm$17 kOe. The rate of the driving magnetic field (dH/dt) was kept constant in order to get a triangular H waveform during the measurement of the hysteresis loops.

Room-temperature dynamic magnetization curves were measured by two custom-built hysteresis loop tracers based on the inductive technique [54]. In both setups, a harmonic driving field capable of magnetizing the sample was generated by a RF coil placed inside one of the two counter-wound pick-up coils designed to measure the inductive magnetic signal. Each hysteresis loop tracer operates in a range of driving field amplitudes and at a frequency appropriate to the specific magnetic material under study. In particular, one setup generates a magnetic field with a frequency of 69 kHz and an amplitude in the range 100–470 Oe and was used to analyse the high-frequency behaviour of typical iron-oxide nanoparticles; the other one operates at a frequency of 20–100 Hz with an amplitude of 1.78 Oe and was used to measure soft magnetic materials such as amorphous ribbons.

VSM setups and custom-built hysteresis loop tracers are typically designed to directly give the $M(H)$ curve. In the measurements done for this work, the sweeping time t was also picked up in order to get the $H(t)$ and $M(t)$ waveforms.

In frequency measurements, the two signals were recorded for a time corresponding to 100 periods of the driving field and processed in frequency by using the discrete Fast Fourier Transform algorithm implemented in the commercial GNU Octave software. In this way the line frequency spectrum of the

magnetization was obtained. The number of periods was such that the spectrum was virtually not affected by the finite time length of the signal.

Quasi-static VSM measurements are typically characterized by an overall time of the experiment of about two hours (the field's period T being of the order of 7200 s). During our measurements the magnetic field was linearly varied with time from the positive maximum field amplitude to the negative one and back, resulting in one full period of a triangular field wave. In order to compare the results obtained using the VSM with the ones obtained from the standard frequency measurements described above, the total sweeping time of the VSM was considered to correspond to the first period of a virtual succession of 100 identical periods, and the variations with time of both M and H recorded during the actual measurement were replicated 100 times. In this way it was possible to implement the harmonic analysis of the $M(t)$ signal under the triangular field wave by making use of the same Fast Fourier Transform algorithm as in actual frequency measurements. Such a method allowed us to obtain a line spectrum of magnetization also in this case.

In the experimental practice, the frequency analysis of periodic magnetization signals characterized by a period of the order of thousands of seconds (as in the case of VSM measurements) is not typically performed, although frequencies as low as about 10 μHz can be investigated by dedicated digital instruments [55]. The procedure developed in this paper was applied to the results of VSM measurements in order to highlight features and flexibility of the proposed mathematical treatment over a wide frequency range.

3. Spectral harmonics and hysteresis loop

The dynamic magnetization $M(t)$ of a magnetic material submitted to a periodic driving field is easily measured from the voltage induced by the sample in a pickup coil placed around or near to the sample [56]. This property can be studied either in the frequency domain (as is the case, e.g. in MPS/MPI) or in the time domain. In the first case, the output of the measurement is the frequency spectrum of magnetization which is a harmonic complex signal, whilst time-resolved measurements allow to get the magnetic hysteresis loop by plotting $M(t)$ as a function of $H(t)$. As a matter of fact, the frequency spectrum and the hysteresis loop contain the same information about the underlying magnetization process, so that they can be considered as equivalent, interchangeable methods for studying the magnetic response of a material, as put in evidence in the next sections. As a consequence, spectral analysis performed through typical setups for signal acquisition and processing can be safely used to study the basic properties of a magnetic material without the need of directly doing magnetic measurements by means of a dedicated instrument such as a VSM or an hysteresis loop tracer.

3.1. Harmonic driving field waveform

We consider a harmonic waveform of the driving field first; with the present choice of the time basis, $H(t)$ is written as:

$$H(t) = H_V \cos(\omega t) \tag{1}$$

where H_V is the maximum field amplitude (also called the *vertex field* of the corresponding hysteresis loop) and $\omega = 2\pi f$, f being the operating frequency. The resulting magnetization $M(t)$ is in general expressed as a Fourier series with only odd harmonics:

$$M(t) = \sum_{n=0}^{\infty} M_{2n+1} \cos\left[(2n+1)\omega t + \phi_{2n+1}\right]. \tag{2}$$

Here, the M_{2n+1} and ϕ_{2n+1} parameters are the amplitudes (moduli) and the phases of the harmonics, as directly derived from spectral analysis. The ϕ's are defined as the phase shifts between each Fourier component of the magnetization spectrum and the sinusoidal $H(t)$ wave. The index n takes all integer values from zero to $+\infty$. Equation (2) can be cast in the equivalent form:

$$M(t) = \sum_{n=0}^{\infty} P_{2n+1} \cos\left[(2n+1)\omega t\right] - \sum_{n=0}^{\infty} Q_{2n+1} \sin\left[(2n+1)\omega t\right] \tag{3}$$

where

$$\begin{aligned} P_{2n+1} &= M_{2n+1} \cos\phi_{2n+1} \\ Q_{2n+1} &= M_{2n+1} \sin\phi_{2n+1}. \end{aligned} \tag{4}$$

The quantities P_{2n+1} and Q_{2n+1} will play a central role in the discussion. An equivalent expression of both parameters is reported in the appendix in the case when it is the frequency spectrum of the voltage induced in a pickup coil which is measured.

It is easy to see that the term ωt of the argument of the sine and cosine functions in equation (3) can be written in each half period of the sinusoidal wave as:

$$\omega t = \arccos(H/H_V) \quad \left[NT \leqslant t \leqslant \left(N+\frac{1}{2}\right) T\right]$$

$$\omega t = 2\pi - \arccos(H/H_V) \quad \left[\left(N+\frac{1}{2}\right) T \leqslant t \leqslant NT\right]$$

where $T = 2\pi/\omega$ is the period and N is an integer positive, negative or zero. Therefore the magnetization M can be expressed as a function of H as:

$$M(H) = \sum_{n=0}^{\infty} P_{2n+1} \cos\left[(2n+1)\arccos(H/H_V)\right] - \sum_{n=0}^{\infty} Q_{2n+1} \sin\left[(2n+1)\arccos(H/H_V)\right] \tag{5}$$

in the upper branch of the hysteresis loop, i.e. when H takes decreasing values from $+H_V$ to $-H_V$ (corresponding to the first half-period of the driving field), and as:

$$M(H) = \sum_{n=0}^{\infty} P_{2n+1} \cos\left[(2n+1)\left(2\pi - \arccos(H/H_V)\right)\right] - \sum_{n=0}^{\infty} Q_{2n+1} \sin\left[(2n+1)\left(2\pi - \arccos(H/H_V)\right)\right] \tag{6}$$

in the lower branch, i.e. when H is increased from $-H_V$ to $+H_V$, corresponding to the second half period of $H(t)$.

3.2. Triangular driving field waveform

A triangular H waveform of period $T = \frac{2\pi}{\omega}$ and maximum amplitude H_V, starting from H_V, can be expressed as:

$$H(t) = \frac{8}{\pi^2} H_V \sum_{m=0}^{\infty} \frac{1}{(2m+1)^2} \cos\left[(2m+1)\omega t\right] \tag{7}$$

The resulting magnetization is always given by equation (3); by elementary geometric considerations the term ωt in each half period of the triangular wave is expressed as a function of H/H_V as:

$$\omega t = \frac{\pi}{2}\ (1 - H/H_V) \qquad \left[NT \leqslant t \leqslant \left(N+\frac{1}{2}\right) T\right]$$

$$\omega t = \frac{\pi}{2}\ (3 + H/H_V) \qquad \left[\left(N+\frac{1}{2}\right) T \leqslant t \leqslant NT\right] \tag{8}$$

N being an integer positive, negative or zero. Therefore, the magnetization M can be expressed as a function of the field H as:

$$M(H) = \sum_{n=0}^{\infty} P_{2n+1} \cos\left[\left(n+\frac{1}{2}\right)\pi\ (1 - H/H_V)\right] - \sum_{n=0}^{\infty} Q_{2n+1} \sin\left[\left(n+\frac{1}{2}\right)\pi\ (1 - H/H_V)\right] \tag{9}$$

in the upper branch of the hysteresis loop, and as:

$$M(H) = \sum_{n=0}^{\infty} P_{2n+1} \cos\left[\left(n+\frac{1}{2}\right)\pi\,(3+H/H_V)\right] - \sum_{n=0}^{\infty} Q_{2n+1} \sin\left[\left(n+\frac{1}{2}\right)\pi\,(3+H/H_V)\right] \quad (10)$$

in the lower branch.

Equations (5) and (6) or (9) and (10) relate M to H for the two commonest driving field waveforms through simple analytic expressions (albeit not cast in closed form) where the coefficients of the double series are derived from the harmonics of the frequency spectrum.

As a matter of fact, determining the relation between M and H in a ferromagnetic material is a difficult task as well as a fascinating mathematical problem which has been approached at different levels of complexity [36]. In the majority of cases no simple analytic expression of the hysteretic $M(H)$ curve can be produced, and the loop properties can be obtained through complex mathematical methods, often involving numerical solutions, such as the Jiles-Atherthon model and the Preisach approach [36, 57]. Only a few exceptions involving explicit analytical solutions exist (e.g. the Rayleigh region of very low fields [58], or the magnetic loops of single-domain particles described by the Stoner-Wohlfarth law at well-defined angles between the easy axis and the magnetic field [59]). The present analysis shows that a simple analytical representation of the loop branches (equations (5) and (6) or (9) and (10)) emerges when the spectral harmonics of the magnetization signal are experimentally known. It should be explicitly noted that the information extracted from the harmonics must be complete, i.e. involving not only the amplitude but also the phase of all significant harmonics of the spectrum. Another analytic formula for $M(H)$ in a loop generated by a sinusoidal driving field, alternative and equivalent to equations (5) and (6), is reported in the appendix. It should be remarked that when a constant term H_0 is added to the oscillating field (equations (1) and (7)), such as for instance in the case of thin films or nanoparticles where a constant exchange-bias field [60] is present, all the previous expressions for the $M(H)$ curves in terms of the spectral harmonics keep their validity with the substitution $H \to (H - H_0)$.

4. Spectral harmonics and basic properties of hysteresis loops

In many applications of magnetic nanoparticles it may be enough to know the value of few basic properties of the hysteretic magnetization. Such properties are the vertex magnetization M_V (i.e. the value of M at the vertex field H_V), and typical parameters such as the hysteresis loop area A_L, the magnetic remanence M_R and the coercive field H_C. In the following, it will be shown that all these properties can be directly derived from spectral analysis without the need of doing time-resolved measurements, and that the relations between spectral harmonics and the hysteretic properties of a material (henceforth called the *transformation formulas*) are indeed very simple. The application-oriented loop parameters depend on the operating amplitude of the ac field, so that changing the field amplitude results each time in a new frequency spectrum to analyse.

4.1. Hysteresis loop's area

The area enclosed by a hysteresis loop plays a central role in biomedical applications, being related to the energy absorbed by the particles from the applied field in one period, which acts to increase their temperature and finally results in a net transfer of heat to the environment. In some cases, as in magnetic hyperthermia [61], such a heat is instrumental to the effectiveness of the therapy and has to be maximized and/or controlled; on the contrary the release of heat can be an unnecessary side effect or even a nuisance in other applications, such as MPI [62], so that in these cases the loop area should be minimized.

The Fourier expressions derived in section 3 can be used to link A_L to the spectral harmonics through simple transformation formulas. When M is plotted as a function of H, the loop's area is by definition:

$$A_L = \oint M \mathrm{d}H.$$

where the integral is on a closed path in the (H,M) plane. Different expressions for A_L apply for sinusoidal or triangular H waveforms.

4.1.1. Harmonic field

When the ac field is harmonic (equation (1)), using time as a parameter and taking into account that $dH = -\omega H_V \sin\omega t dt$, one gets

$$A_L = \oint M dH = -\omega H_V \int_0^T M(t) \sin\omega t dt.$$

where $M(t)$ is given by the double Fourier series of equation (3). Exploiting the orthogonality of the Fourier basis functions and calling $x = \omega t$ (whence the upper integration limit becomes 2π) it turns out that only the integral $\int_0^{2\pi} \sin(2n+1)x \sin x dx$ with $n = 0$ has a nonzero value, so that the loop area turns out to be simply expressed by:

$$A_L = H_V Q_1 \int_0^{2\pi} \sin^2 x dx = \pi H_V Q_1. \tag{11}$$

where $Q_1 = M_1 \sin\phi_1$, M_1 and ϕ_1 being the amplitude and phase of the first harmonic, respectively. Therefore, for a sinusoidal H waveform modulus and phase of the first harmonic of M obtained by spectral analysis are enough to get the loop's area.

4.1.2. Triangular field

When the ac field has triangular waveform (equation (7)), the differential element dH can be written as:

$$dH = -\frac{8}{\pi^2} H_V \omega \sum_{m=0}^{\infty} \frac{1}{(2m+1)} \sin\left[(2m+1)\omega t\right] dt, \tag{12}$$

so that using again equation (3) and exploiting the orthogonality of the Fourier basis function, one gets:

$$\begin{aligned} A_L &= \frac{8}{\pi^2} H_V \omega \sum_{n=0}^{\infty} \frac{Q_{2n+1}}{(2n+1)} \int_0^T \sin^2\left[(2m+1)\omega t\right] dt \\ &= \frac{8}{\pi^2} H_V \sum_{n=0}^{\infty} \frac{Q_{2n+1}}{(2n+1)} \int_0^{2\pi} \sin^2\left[(2m+1)x\right] dx \\ &= \frac{8}{\pi} H_V \sum_{n=0}^{\infty} \frac{Q_{2n+1}}{(2n+1)} = \frac{8}{\pi} H_V \left[\frac{Q_1}{1} + \frac{Q_3}{3} + \frac{Q_5}{5} + \ldots\right]. \end{aligned} \tag{13}$$

Therefore, all odd harmonics obtained by spectral analysis are needed to determine the loop's area in the case of triangular field waveform.

It should be explicitly noted that both transformation formulas for A_L (equations (11) and (13)) involve the quantities $Q_{2n+1} (\propto \sin\phi_{2n+1})$ only. This is explained recalling that a magnetic hysteresis loop appears when the harmonics of M are shifted by a generic phase angle with respect to the driving field. When all harmonics of M are either in phase ($\phi = 0$) or in opposition ($\phi = \pi$) with the driving field, the loop area is exactly equal to zero, i.e. the $M(H)$ curve displays no hysteresis, as in the very special (and unlikely) case of superparamagnetic particles whose magnetization can still be described by a Langevin function at the operating frequency [38, 40].

4.2. Main hysteresis loop parameters

- The magnetization at the positive vertex field (M_V) is immediately derived from equation (3) by simply taking $t = 0$. Therefore,

$$M_V = \sum_{n=0}^{\infty} P_{2n+1} = \left[P_1 + P_3 + P_5 + \ldots\right]. \tag{14}$$

  Of course the magnetization at the negative vertex of a symmetric loop is just $-M_V$. This transformation formula applies to both harmonic and triangular waveform.
- The magnetic remanence (M_R) is the value taken by the magnetization at $H = 0$. For both considered driving field waveforms, H is equal to zero when $t = (N + 1/4)\pi$ and $t = (N + 3/4)\pi$ (where N is again an integer positive, negative or zero). Therefore, the positive/negative magnetic remanence are immediately obtained from equation (3) by taking into account that in both cases all cosine terms in the double series are equal to zero and the sine terms alternatively take the value ± 1, resulting in the following transformation formula:

$$\pm M_R = \pm \sum_{n=0}^{\infty} (-1)^{2n} Q_{2n+1} = \pm \left[Q_1 - Q_3 + Q_5 - \ldots\right]. \tag{15}$$

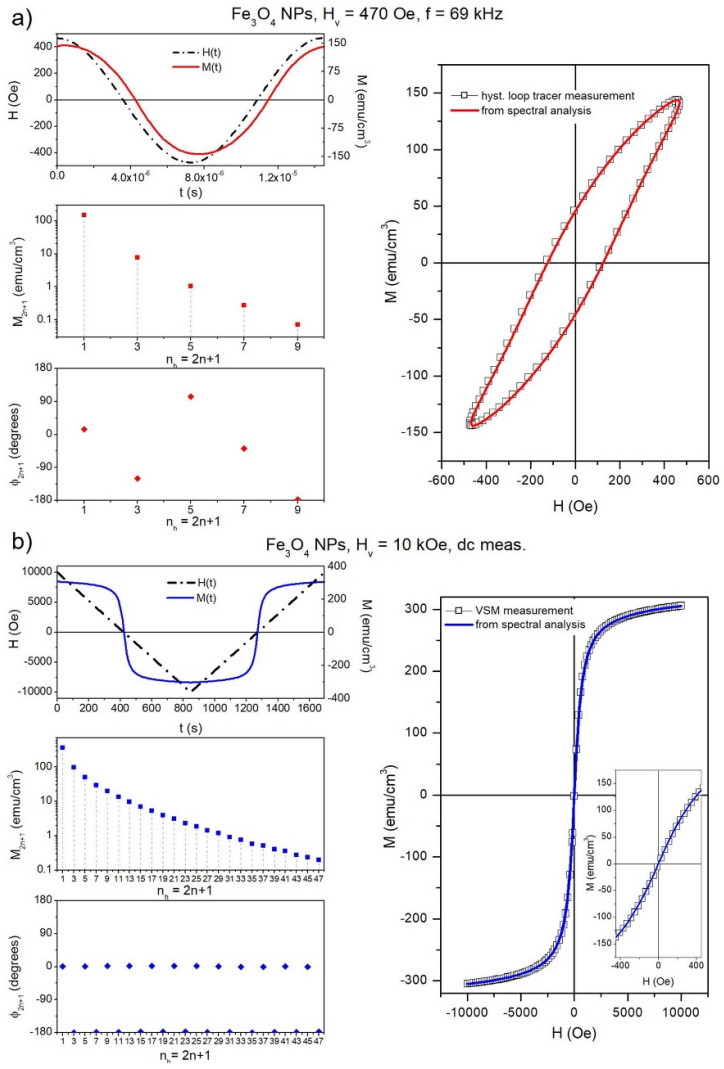

Figure 1. Panel (a)—top left frame: $H(t)$ and $M(t)$ waveforms for magnetite nanoparticles at $f = 69$ kHz; centre/bottom left frames: amplitudes and phases of the significant spectral harmonics of magnetization; right frame: hysteresis loop at the same frequency (open symbols: measurement; full line: reconstruction from spectral harmonics. Panel (b): the same as in (a) for the same magnetite nanoparticles measured in quasi-static conditions.

- The negative/positive coercive fields (i.e. the fields where the hysteretic magnetization is equal to zero) are obtained by requiring that the right-side members of equations (5) and (6) (sinusoidal H waveform) and equations (9) and (10) (triangular H waveform) be equal to zero. When the measured spectrum includes harmonics up to the $(2n+1)$th order, it can be checked that the solution for H_C is obtained by solving an algebraic equation of degree $(2n+1)$ in $(H/H_V)^2$. As a consequence, no analytical solution can be found for odd $n > 1$, and the equation has to be numerically solved. In contrast, for nearly elliptical minor hysteresis loops where all harmonics with $n > 1$ (i.e. beyond the third harmonic) are negligible H_C can be obtained in closed form, as shown in the appendix.

5. Experimental check of the theory

The simple transformation formulas developed in sections 3 and 4 can be experimentally checked by measuring in both time and frequency domains the dynamic magnetization of magnetic materials belonging to markedly different classes, having different size, and being submitted to driving fields of different waveform, magnitude and frequency. All measurements were done at room temperature.

5.1. Hysteresis loop reconstruction

The ability of equations (5), (6) or (9), (10) to reconstruct the hysteresis loop branches on the basis of the knowledge of the harmonics of the $M(t)$ signal is checked in figure 1 for a dried powder of magnetite nanoparticles.

Panel (a) shows the magnetic behaviour of the sample submitted to a harmonic magnetic field of frequency 69 kHz and maximum amplitude 470 Oe. These field parameters are of the same order of magnitude as the ones used in present-day techniques of magnetic hyperthermia, imaging and spectroscopy [20, 21, 63]. The top left frame shows one full period of both $H(t)$ and $M(t)$ signals, as generated and measured by a hysteresis loop tracer. The amplitudes M_{2n+1} of the harmonics obtained from spectral analysis of the $M(t)$ signal are reported in the centre left frame, while the bottom left frame shows the corresponding phases ϕ_{2n+1}. The results are plotted as functions of the harmonic number $n_h = 2n + 1$; n_h takes all positive odd integer values from 1 to $+\infty$. In the present case, the $M(t)$ signal is not much deformed from a sinusoidal curve, so that only five harmonics of the frequency spectrum are significant (i.e. distinctly above the background noise). Note also that the phases are in general different from either zero or π, indicating a hysteretic behaviour of the cyclic magnetization process. This is actually shown in the right frame, where the measured $M(H)$ loop obtained from the time-resolved signals is reported (open symbols). It should be explicitly noted that this is a typical example of *frequency-sustained* magnetic hysteresis, as it will become apparent by comparison with the results in dc conditions. The red line shows the loop as reconstructed from the harmonics obtained by frequency analysis, using equations (5) and (6) for the upper/lower branch of the loop, respectively. The P_{2n+1} and Q_{2n+1} coefficients were generated from the M_{2n+1} and ϕ_{2n+1} values reported in the left-side frames. The agreement between the two curves is excellent.

Panel (b) shows the cyclic magnetization of the same sample measured in dc conditions by a VSM setup. In this case, the magnetic field waveform is triangular instead of sinusoidal and its frequency is basically zero. The maximum field amplitude was set to 1×10^4 Oe in order to approach magnetic saturation. The top left frame shows again one full period of the $H(t)$ wave generated by the VSM as well as the resulting $M(t)$ wave, which turns out to be severely deformed from the triangular wave. The amplitudes and phases of the harmonics obtained from spectral analysis of the $M(t)$ signal are again reported in the centre and bottom left frames. In the present conditions the number of significant harmonics turns out to be much higher than in the previous measurement (panel (a)). All phases are now either zero or π, indicating that the $M(t)$ signal—albeit deformed—in still in phase with $H(t)$, so that the magnetization is expected to be an anhysteretic function of H. This is checked in the right frame where the experimental $M(H)$ curve is reported (open symbols); the blue line shows the reconstruction done using equations (9) and (10) appropriate to the triangular H waveform; the curves for the two branches turn out to be exactly superimposed. Once again theoretical curves and experimental data are perfectly matching.

The inset in the right frame of panel (b) shows the region around zero field of the $M(H)$ curve, measured by VSM with a much lower vertex field ($H_V \approx 470$ Oe). The absence of magnetic hysteresis in both theoretical and experimental curves is confirmed, indicating that the magnetite nanoparticles measured in this work can be properly considered as SPION [41], being superparamagnetic at room temperature and characterized by a $M(H)$ curve which follows the Langevin law [56]. The inset can be compared with the right frame of panel (a), showing the $M(H)$ behaviour in the very same field range but at high frequency: the comparison shows that magnetic hysteresis can emerge in SPION submitted to a driving field of sufficiently high frequency. When the magnetization is analysed in the frequency domain, the insurgence of frequency-sustained hysteresis can be easily and quickly checked by looking at the behaviour of the *phases* of the spectral harmonics.

Figure 2 shows other two examples of reconstruction of the hysteresis loop, done using the same scheme as in figure 1. The magnetic materials were chosen because the are markedly different in size and properties from typical SPION. In panel (a) the loop reconstruction method is applied to a dried powder of Co-Zn ferrite grains (composition: $Co_{0.84}Zn_{0.16}Fe_2O_4$), a material with large coercive field and loop area, magnetically *harder* [59] than iron-oxide nanoparticles (both hysteretic and SPIONs); panel (b) refers to a macroscopic piece cut from an amorphous metallic ribbon (composition: $Fe_{62.50}$ $Ni_{10.00}$ $Si_{11.05}Cr_{2.23}B_{11.14}C_{3.09}$), which is an extremely soft magnetic material with coercive field almost three orders of magnitude lower than the one of hysteretic iron-oxide NPs, and can be used in sensors for bioapplications.

The measurements on Co-Zn ferrite were done in dc conditions using a VSM and a triangular H wave with maximum value of 7.5 kOe; the resulting hysteresis loop (open symbols in the right frame of panel (a)) is a *major* loop, i.e. it is characterized by a vertex field well above the so-called closure field, which is where the two loop's branches become superimposed and the magnetization process becomes reversible. On the other hand, the measurements on the amorphous ribbon were done at 20 Hz using a sinusoidal H field of maximum amplitude 1.78 Oe: such a value is enough to bring the material close to saturation and to obtain a major hysteresis loop as well (open symbols in the right frame of panel (b)). In both cases, the number of significant harmonics in the frequency spectrum of M is high (centre left frames in both panels) and the phases are in general different from zero or π (bottom left frames). The reconstructed loops (lines in colour in the two frames to the right) are perfectly superimposed to the experimental curves.

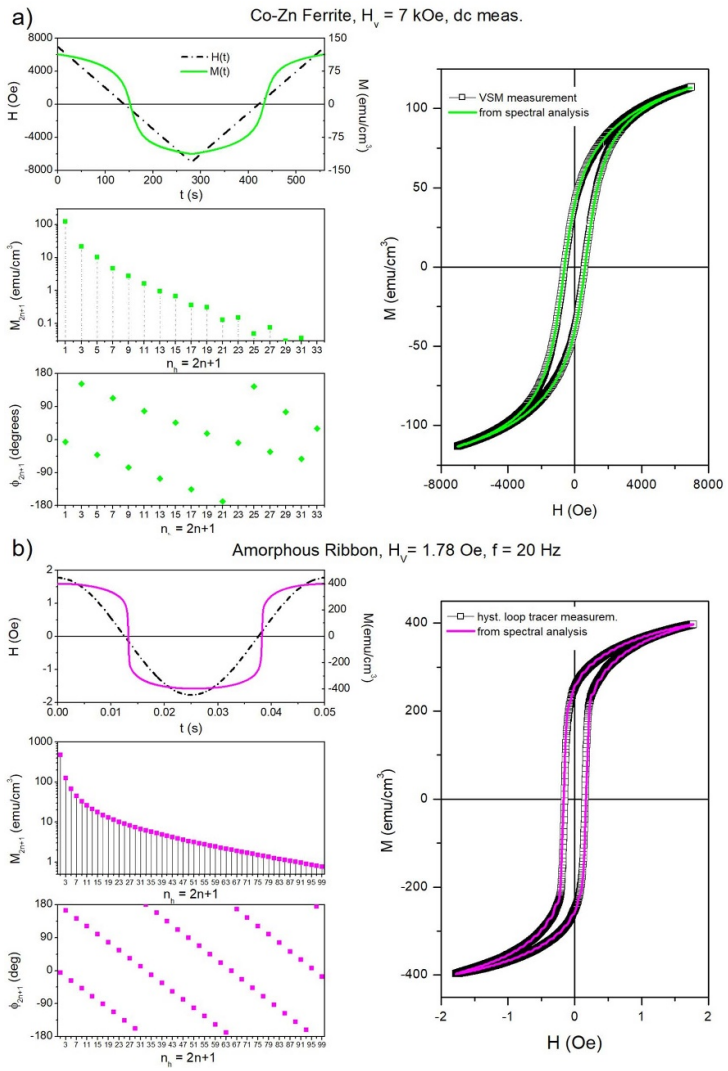

Figure 2. Panel (a)—top left frame: $H(t)$ and $M(t)$ waveforms for Co-Zn ferrite particles measured in quasi-static conditions; centre/bottom left frames: amplitudes and phases of the significant spectral harmonics of magnetization; right frame: dc hysteresis loop (open symbols: measurement; full line: reconstruction from spectral harmonics). Panel (b): the same as in (a) for an amorphous magnetic ribbon of composition $Fe_{62.50}\ Ni_{10.00}\ Si_{11.05}Cr_{2.23}B_{11.14}C_{3.09}$ at 20 Hz.

In spite of the strong differences existing among the magnetic materials studied in this section as well as among the measuring setups and the experimental conditions, hysteresis loop reconstruction from the spectral harmonics is always fully satisfactory.

5.2. Hysteresis loop parameters

The simple transformation formulas of section 4, relating basic magnetic properties and spectral harmonics, are shown here to precisely reproduce the experimental data. An example is given in figure 3, where experimental values taken from the hysteresis loops are compared with the expressions obtained from spectral analysis for the samples containing magnetite nanoparticles and Co-Zn ferrite grains.

In magnetic materials the four quantities A_L, M_V, M_R, H_C are monotonically increasing functions of the vertex field from zero up to the closure field [58, 59]. A set of hysteresis loops were produced by properly increasing H_V in the two considered samples without changing the driving-field frequency.

The experimental behaviour of A_L (open symbols in panels (a) and (b)) is almost linear in the H_V range 150–470 Oe and at $f = 69$ kHz (sinusoidal wave), i.e. in the typical conditions of MPS/MPI and magnetic hyperthermia (left-side panel); for the Co-Zn ferrite characterized by VSM with triangular H wave, the range of field amplitude values was much wider (1×10^2 to 7×10^3 Oe), and A_L approaches the asymptotic maximum at high fields. The experimental results for $A_L(H_V)$ are well reproduced by the relevant transformation formulas (equations (11) and (13), respectively; full symbols in colour).

The coercive field is a particularly important parameter in applications because it gives a quick estimate of the amplitude of the magnetic field needed to switch the magnetization of a magnetic material. The

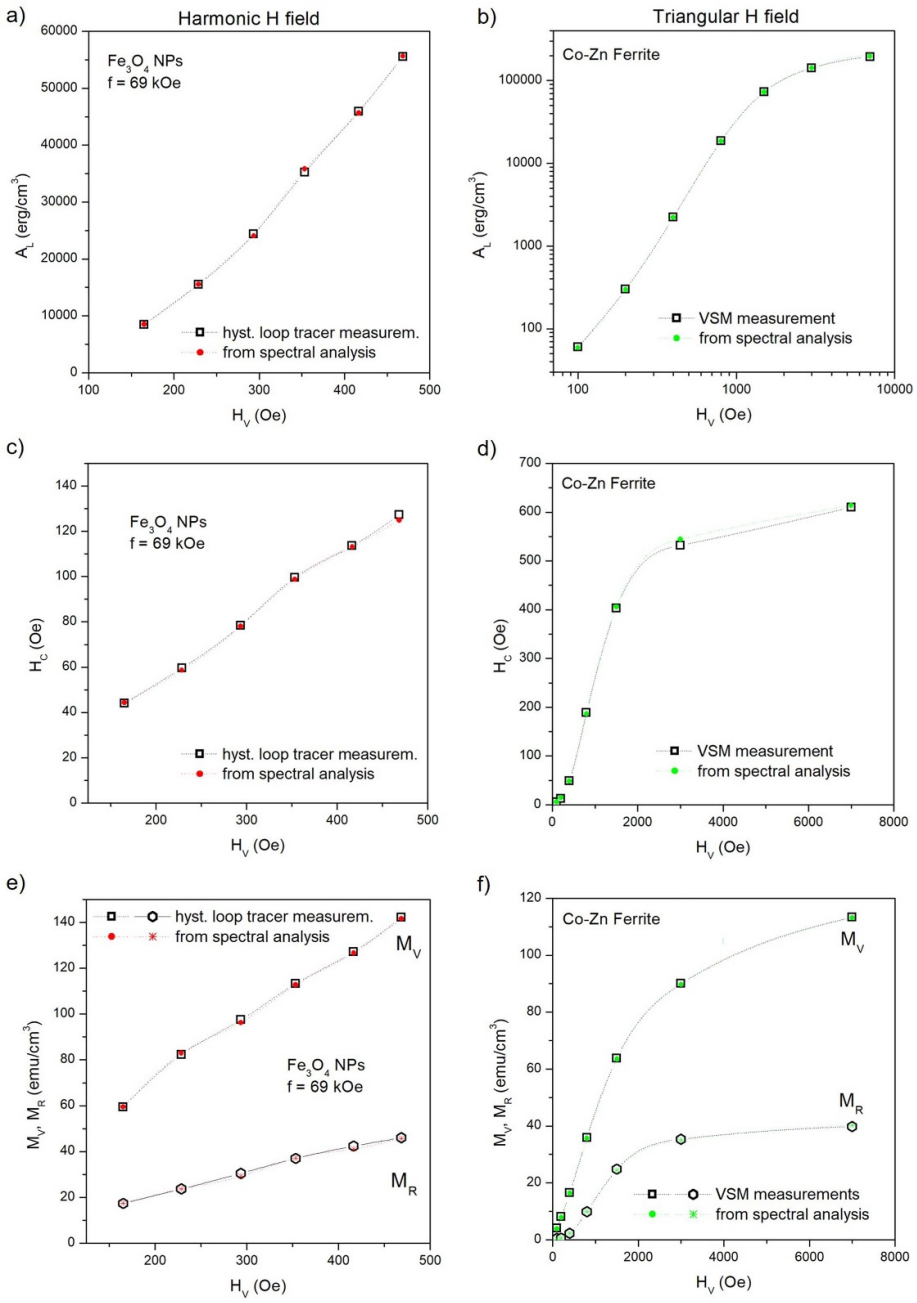

Figure 3. Agreement between measured and reconstructed hysteresis loop's parameters for magnetite nanoparticles at $f = 69$ kHz and for Co-Zn ferrite particles measured in quasi static conditions: (a) and (b) hysteresis loop's area, (c) and (d) coercive field; (e) and (f) vertex magnetization and magnetic remanence.

notable agreement between measured coercive field and the values obtained from equations (5)–(10) is shown in panels (c) and (d) (open / full symbols, respectively).

A similar agreement is shown in panels (e) and (f) for vertex magnetization (M_V) and remanence (M_R). Both properties play important roles in many recent applications of magnetic materials: the vertex magnetization is proportional to the amplitude of the induced voltage signal and can therefore be used to determine, for a given magnetic nanomaterial, the minimum concentration needed to get a measurable signal [64]; on the other hand, magnetic remanence of nanoparticles is very sensitive to physical and chemical effects such as dipole-dipole interactions among distant particles, magnetic contact interactions and magnetic coherence length [65] in aggregated particles, interfacial coupling between particles and non-magnetic entities, such as molecules decorating the particle surface and/or functionalization agents [66], and can therefore be used to monitor changes with time of nanoparticle concentration, degree of aggregation, surface coverage both *in vitro* and *in vivo*.

The present results confirm that spectral analysis of the $M(t)$ signal permits to accurately derive the most useful parameters of the hysteresis loop by applying the transformation formulas. As a practical example of the interplay between time and frequency representations of the magnetization process, the following section is devoted to a study of biocompatible ferromagnetic nanodiscs.

6. A study case: permalloy ($Ni_{80}Fe_{20}$) nanodiscs for biomedical applications

An enlightening example of the interplay between hysteresis loop measurements and magnetic spectroscopy of nanomaterials is provided by a combined study of metallic nanodiscs containing a film of $Ni_{80}Fe_{20}$ (permalloy, a soft ferromagnetic material) and developed for biomedical applications [53].

VSM measurements on nanodiscs were performed using a triangular $H(t)$ waveform of period $T \approx 7.2 \times 10^3$ s and maximum field amplitude $H_V = 2$ kOe, enough to magnetically saturate the films. When the nanodiscs were still attached on the substrate the field was applied in the film plane; in the case of water dispersion, the angle between the normal to each nanodisc and the field direction dynamically varied with time during the measurement; in fact, a simple calculation shows that the typical relaxation time for the rotation of 630 nm nanodiscs is much faster than the measurement time, being of the order of 0.1 s in water at room temperature.

The hysteresis loops, normalized to the saturation magnetization, are shown in panels (a) and (b) of figure 4 (open symbols). Both loops have a peculiar shape, characterized by two open lobes at intermediate fields (regions of large magnetic irreversibility) and by exceedingly small remanence and coercive field, making the $M(H)$ curve almost anhysteretic around $H = 0$ [1]. These features clearly point to the presence of a vortex state of the magnetization at zero field [53, 67], with nucleation and annihilation processes involving asymmetric field intervals. In nanodiscs suspended in water (panel (b)), the magnetization jumps corresponding to nucleation and annihilation of the vortex are less pronounced than the ones measured when the discs were still attached to the substrate (panel (a)). Such a smoothing effect is ascribed to the random rotation of the normal to the disc plane with respect to the applied field [53, 68]. In this case the overall magnetic response is thought to be a superposition of intrinsic effects (i.e. rearrangements of the magnetization vector in each permalloy film) and effects arising from the random rotation of nanodiscs because of thermal disorder, similar to Brownian relaxation in magnetic nanoparticles [43].

Spectral analysis of the time-resolved magnetization signals is shown in panels (c) and (d) of figure 4. Even in this case, reconstruction of hysteresis loops through equation (9) using the experimental M_{2n+1} and ϕ_{2n+1} parameters is able to reproduce all details of the measured $M(H)$ curves, as shown by the lines in colour in panels (a) and (b). Spectral analysis helps to get more insight on the physics of the magnetization process in the samples; in fact, the most interesting features of the frequency spectrum of $M(t)$ are the following:

- the spectral amplitudes of the two samples are almost the same for the lowest n_h values (basically, up to $n_h = 7$); this means that in the present case the analysis of specific low-harmonic ratios such as M_5/M_3, often exploited in MPS studies of nanoparticles [21], would not be enough to distinguish between the effects of different environments on nanodiscs;
- at first glance, a marked difference emerges between the behaviour with n_h of the amplitudes M_{2n+1} of the two samples: the $M_{2n+1}(n_h)$ curve is smooth and regular, while a well-defined structure (a dip) appears at intermediate n_h values in the behaviour of the harmonics of blocked nanodiscs; beyond the dip, the two curves merge again, the differences between them at very high n being considered not significant;
- a similar difference is observed between the phases ϕ_{2n+1}: in blocked nanodiscs, the phase angles evolve rather regularly between $-180°$ and $+180°$, an anomaly appearing for n_h values which correspond to the dip of the amplitudes; on the contrary, the phases of nanodiscs dissolved in water alternatively take values always very close to either zero or $\pm 180°$, a behaviour similar to the one of superparamagnetic particles which follow the Langevin law, where the phases exactly take values exactly equal to zero and $\pm 180°$ (see for instance figure 1, lower left frame of panel (b)).

The dip in the spectral harmonics observed in blocked nanodiscs corresponds to processes occurring in the 100–400 s time range, which is compatible with vortex nucleation by effect of the triangular magnetic field (which takes place in ≈100 s in the present experimental conditions) as well as vortex annihilation, taking place in ≈400 s (see supplementary material). In the frequency interval corresponding to the dip the power associated to the magnetization process is reduced with respect to the case of suspension in water, a fraction

[1] In the ideal case, both remanence and coercive field are exactly equal to zero.

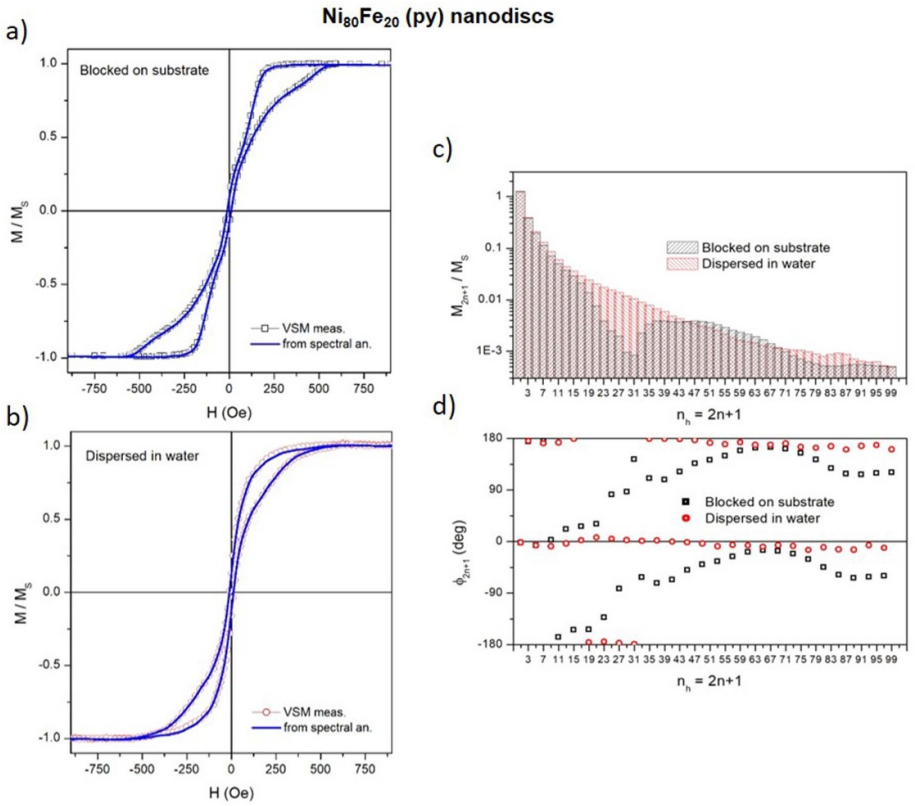

Figure 4. Panels (a) and (b): hysteresis loops measured on permalloy nanodiscs in quasi static conditions; (a) nanodiscs still attached to the substrate; (b) nanodiscs dispersed in water; panels (c) and (d): comparison between the amplitudes and phases of the spectral harmonics for blocked and dispersed nanodiscs.

of power being absorbed by processes presumably connected with vortex nucleation/annihilation. As vortex nucleation and annihilation occur in both samples [53], the dip must be related to the particular arrangement of nanodiscs when they are still attached to the substrate; interfacial effects between nanodiscs and substrate are supposed to play some role in the process.

On the other hand, the behaviour of the ϕ's for nanodiscs suspended in water is clearly ascribed to the dynamic disordering effect of the fluid environment, which makes such a system analogous to a superparamagnetic material.

As a final remark, in both samples the amplitude of the first harmonic normalized to M_s (panel (c) of figure 4) is larger than 1; this implies that the first harmonic of the magnetization is larger than the maximum magnetization of the sample. Such a counterintuitive result has been explained elsewhere [40] and is related to the alternate signs of the P_{2n+1} coefficients. The vertex magnetization, which in this case corresponds to the saturation magnetization (see figure 4) is given by the sum $\sum P_{2n+1}$ and is therefore affected by the alternate sign of the P's. In particular, the sum over all terms turns out to be lower than the first term of the sum ($P_1 \approx M_1 = 1.25\ M_S$ and $1.27\ M_S$ in blocked and suspended nanodiscs, respectively).

The example of ferromagnetic nanodiscs shows that combining the spectral analysis of magnetization with conventional magnetic measurements allows to grasp the complexity of the behaviour of a magnetic nanomaterial in different environments. In fact, the difference in the magnetic behaviour of a nanomaterial arising from different surroundings may be effectively put in evidence by associating spectral analysis to the measurement of hysteresis loops. Moreover, spectral analysis has been shown to be a particularly powerful way to interpret certain features of the magnetization signal on the basis of physical grounds.

7. Conclusions

We have shown that detection techniques used in MPS/MPI can be exploited to easily get a complete picture of the actual magnetic behaviour of magnetic nanomaterials for bioapplications,

The cyclic behaviour of biocompatible magnetic nanomaterials submitted to an ac magnetic field is in general characterized by magnetic hysteresis effects, which are often disregarded (and their consequences

underestimated) in all applications where magnetic nanomaterials are operated at high frequency. The point is that the characteristic features of the hysteresis loops—such as width and shape—and their most important application-oriented parameters—such as magnetic remanence, coercive field, loop's area—are inherently dependent on a variety of factors including the nature of the nanomaterial's environment, the surface functionalization, the degree of interaction and aggregation among magnetic nanoelements, the frequency and amplitude of the driving field. A sine qua non for the success of any specific therapy or imaging technique based on biocompatible nanomaterials is therefore to get an accurate picture of the true magnetic behaviour of the material in the actual operating conditions.

The information currently extracted from the frequency spectra of magnetization is interesting but often far from exhaustive, so that conventional magnetic measurements are typically needed to complement the frequency analysis, because the evolution of the environment's conditions is reflected in a more insightful way by the changes of the application-oriented parameters of hysteresis loops. The model presented in this paper provides an important link, both conceptual and practical, between frequency analysis and conventional magnetic measurements, making it possible to avoid the need of actually doing the latter.

In fact, the inherent difficulty of associating standard magnetic measurements to magnetic spectroscopy is removed by taking into account that the same amount of information on the magnetization process is gained by performing measurements either in the time domain or in the frequency domain. Magnitude and phase of the odd harmonics resulting from spectral analysis of the dynamic magnetization $M(t)$ (or alternatively of the voltage $V(t)$ induced in a pickup coil) contain a complete information about the magnetization process in the nanomaterial and allows the user to easily reconstruct the actual hysteresis loop under the most common driving-field waveshapes.

The reconstructed hysteresis loops obtained through spectral analysis have been proven to accurately reproduce all features and details of the ones observed through standard magnetic measurements in the time domain, independently of the value of the vertex field and of the actual loop shape. In addition, the simple transformation formulas proposed in this work will allow the user to directly calculate the most important parameters of the loop from amplitude and phase of the odd harmonics of the magnetization. It is important to remark that the power spectrum and the amplitude spectrum of the magnetization signal, by themselves, are not sufficient to correctly derive the magnetic parameters of interest: in fact, the phases of the measured harmonics play a role as important as the amplitudes in the transformation formulas.

The transformation formulas developed in this paper apply to the case of magnetization curves which are *symmetrical* with respect to the origin of the axes in the (H, M) plane. In general, the method cannot be applied to describe $M(H)$ curves characterized by some asymmetry (such as, for instance, minor loops not centred in the origin and the results of FORC measurements), with the exception of hysteresis loops in the presence of an exchange bias field, as already remarked.

Finally, spectral analysis not only provides information about the dynamic magnetization of a nanomaterial submitted to an ac magnetic field, including the amount of hysteresis characterizing the cyclic process, but is also useful to ascertain the physical effects underlying the magnetization process of the material. Properly complementing hysteresis loop observation with spectral harmonic analysis is the key to get a satisfactory picture of the magnetization process, which is instrumental to optimize the performance of a magnetic nanomaterial in bioapplications.

Data availability statement

All data that support the findings of this study are included within the article (and any supplementary files).

Acknowledgments

The Authors thank Dr R Busch and Dr I Gallino of the Saarland University, Saarbrücken for kindly providing the amorphous ribbon and Dr E Ferrara of INRIM, Torino for doing the magnetic measurements on the same ribbon.

Appendix

Transformation formulas for the voltage induced in a pickup coil

The frequency spectrum of the voltage $V(t)$ induced in a pickup coil can be directly used to get information on the magnetic properties without the need of integrating the picked-up signal. Keeping in mind that

$$V(t) = -S\frac{\mathrm{d}B}{\mathrm{d}t} \approx -S\frac{\mathrm{d}M}{\mathrm{d}t}$$

where S is the effective cross section of the pickup coil, the expansion for $V(t)$ equivalent to equation (2) is:

$$V(t) = \sum_{n=0}^{\infty} V_{2n+1} \cos\left[(2n+1)\omega t + \phi_{2n+1}^{(V)}\right]. \tag{16}$$

where the V_{2n+1}'s and $\phi_{2n+1}^{(V)}$'s are the amplitudes (moduli) and the phases of the harmonics of the induced-voltage spectrum, related to the equivalent quantities for the magnetization by:

$$\begin{aligned} V_{2n+1} &= (2n+1)\,\omega S M_{2n+1} \\ \phi_{2n+1}^{(V)} &= \phi_{2n+1} - \frac{\pi}{2}. \end{aligned} \tag{17}$$

Therefore the P_{2n+1}, Q_{2n+1} coefficients entering all transformation formulas used in this work are directly expressed in terms of the induced-voltage harmonics as:

$$\begin{aligned} P_{2n+1} &= -\frac{1}{(2n+1)\,\omega S} V_{2n+1} \cos\phi_{2n+1}^{(V)} \\ Q_{2n+1} &= -\frac{1}{(2n+1)\,\omega S} V_{2n+1} \sin\phi_{2n+1}^{(V)}. \end{aligned} \tag{18}$$

Alternative analytical expression for $M(H)$

Equations (5) and (6) describe the upper/lower branch of a $M(H)$ hysteresis loop under a sinusoidal driving field. An alternative expression involving increasing powers of the field is derived here. Using $\cos(\omega t) = h$ where $h = H/H_V$ and exploiting the representation of trigonometric functions of multiples of the argument in terms of powers of these functions, equations (5) and (6) can be recast as:

$$\begin{aligned} M(t) = {} & P_1 h \pm Q_1(1-h^2)^{1/2} + P_3\left[4h^3 - 3h\right] \pm Q_3\left[3(1-h^2)^{1/2} - 4(1-h^2)^{3/2}\right] \\ & + P_5[16h^5 - 20h^3 - 5h] \pm Q_5[5(1-h^2)^{1/2} - 20(1-h^2)^{3/2} + 16(1-h^2)^{7/2}] + \ldots \end{aligned} \tag{19}$$

where the plus/minus signs refer to the upper/lower loop branch. Equation (19) can be further modified by grouping all terms containing the same power of $h = H/H_V$ and $(1-h^2)^{1/2}$:

$$M(H) = \sum_{n=0}^{\infty} C_{2n+1}(H/H_V)^{2n+1} \pm \sum_{n=0}^{\infty} D_{2n+1}[1-(H/H_V)^2]^{2n+1} \tag{20}$$

where the plus/minus signs again refer to the upper/lower loop branch and the general expressions of the C_{2n+1}, D_{2n+1} coefficients in terms of the quantities P_{2n+1} and Q_{2n+1} are:

$$C_{2n+1} = 2^{2n}\left[P_{2n+1} + \frac{1}{(2n+1)!}\sum_{k=n+1}^{\infty}(-1)^{k-n}\frac{2k+1}{k-n}\frac{(k+n)!}{(k-n-1)!}P_{2k+1}\right] \tag{21}$$

and:

$$D_{2n+1} = (-1)^n\ 2^{2n}\left[Q_{2n+1} + \frac{1}{(2n+1)!}\sum_{k=n+1}^{\infty}\frac{2k+1}{k-n}\frac{(k+n)!}{(k-n-1)!}Q_{2k+1}\right] \tag{22}$$

Equation (20), fully equivalent to equations (5) and (6), is an analytical expression of the hysteretic $M(H)$ curve of a generic magnetic material submitted to a harmonic driving field of maximum amplitude H_V and arbitrary frequency in terms of powers of the field, involving only quantities obtained from frequency analysis of magnetization.

Analytic expression for H_C for nearly elliptical loops

When all harmonics of $M(t)$ beyond the first one are completely negligible, the corresponding hysteresis loop has a perfectly elliptical shape. Actual minor loops measured on magnetic nanomaterials using fields of low amplitude are often characterized by a shape slightly deformed from the ellipse; in such an instance, only the first and the third harmonic are present all higher-order terms being negligible.

In this case that the coercive field can be obtained in closed form from equation (20) by solving the cubic equation $ax^3 + bx^2 + cx + d = 0$ for $x = h^2 = (H/H_V)^2$ where:

$$\begin{aligned} a &= C_3^2 + D_3^2 \\ b &= \left[2C_1C_3 - D_3^2 - 2D_3(D_1 + D_3)\right] \\ c &= \left[C_1^2 + 2D_3(D_1 + D_3) + (D_1 + D_3)^2\right] \\ d &= -(D_1 + D_3)^2, \end{aligned} \tag{23}$$

the $C_{1,3}$ and $D_{1,3}$ quantities being obtained from equations (21) and (22). In particular:

$$\begin{aligned} C_1 &= P_1 - 3P_3 \\ C_3 &= -4P_3 \\ D_1 &= Q_1 + 3Q_3 \\ D_3 &= 4Q_3. \end{aligned} \tag{24}$$

The $P_{1,3}$ and $Q_{1,3}$ parameters were defined in equation (4). It can be easily checked that the cubic equation for x has one (and only one) real positive root. Finally, the positive and negative coercive fields are obtained by taking the square root of the solution.

ORCID iD

Gabriele Barrera https://orcid.org/0000-0002-3174-8092

References

[1] Park W, Shin H, Choi B, Rhim W K, Na K and Keun Han D 2020 *Prog. Mater. Sci.* **114** 100686
[2] Seal P, Saikia D and Borah J P 2021 Magnetic nanomaterials and their biomedical applications *Nanostructured Materials and Their Applications* (*Materials Horizons: From Nature to Nanomaterials*) (Singapore: Springer) pp 81–97
[3] Del Sol-Fernández S, Martínez-Vicente P, Gomollón-Zueco P, Castro-Hinojosa C, Gutiérrez L, Fratila R M and Moros M 2022 *Nanoscale* **14** 2091–118
[4] Liu X *et al* 2022 *Prog. Biomed. Eng.* **4** 012005
[5] Wu K, Su D, Liu J, Saha R and Wang J P 2019 *Nanotechnology* **30** 1–47
[6] Krasia-Christoforou T, Socoliuc V, Knudsen K D, Tombácz E, Turcu R and Vékás L 2020 *Nanomaterials* **10** 1–67
[7] Zanker A A, Stargardt P, Kurzbach S C, Turrina C, Mairhofer J, Schwaminger S P and Berensmeier S 2022 *Biotechnol. J.* **17** 1–12
[8] Gambhir R P, Rohiwal S S and Tiwari A P 2022 *Appl. Surf. Sci. Adv.* **11** 100303
[9] Bilal M, Iqbal H M, Adil S F, Shaik M R, Abdelgawad A, Hatshan M R and Khan M 2022 *J. Adv. Res.* **38** 157–77
[10] Albinali K E, Zagho M M, Deng Y and Elzatahry A A 2019 *Int. J. Nanomed.* **14** 1707–23
[11] Chen K L, Yang Z Y and Lin C W 2021 *J. Nanobiotechnol.* **19** 1–11
[12] Ma M, Zhu H, Ling J, Gong S, Zhang Y, Xia Y and Tang Z 2020 *ACS Nano* **14** 4036–44
[13] Wei R, Xu Y and Xue M 2021 *J. Mater. Chem.* B **9** 1965–79
[14] Kralj S and Marchesan S 2021 *Pharmaceutics* **13** 1262
[15] Liu D, Li S, Zhang T, Jiang H and Lu Y 2021 *ACS Appl. Mater. Interfaces* **13** 36157–70
[16] Divieto C *et al* 2020 *Front. Nanotechnol.* **2** 1–14
[17] Bariwal J, Ma H, Altenberg G A and Liang H 2022 *Chem. Soc. Rev.* **51** 1702–28
[18] Garcés V, González A, Gálvez N, Delgado-López J M, Calvino J J, Trasobares S, Fernández-Afonso Y, Gutiérrez L and Dominguez-Vera J M 2022 *Nanoscale* **14** 5716–24
[19] Veloso S R *et al* 2022 *Nanoscale* **14** 5488–500
[20] Harvell-Smith S, Tunga L D and Thanh N T K 2021 *Nanoscale* **14** 3658–97
[21] Wu K, Su D, Saha R, Liu J, Chugh V K and Wang J-P 2020 *ACS Appl. Nano Mater.* **3** 4972–89
[22] Nikitin P I, Vetoshko P M and Ksenevich T I 2007 *J. Magn. Magn. Mater.* **311** 445–9
[23] Hou Y and Sellmyer D J 2017 *Magnetic Nanomaterials* (Weinheim: Wiley-VCH Verlag GmbH & Co. KGaA)
[24] Ludwig F, Balceris C, Jonasson C and Johansson C 2017 *IEEE Trans. Magn.* **53** 55–58
[25] Moor L, Scheibler S, Gerken L, Scheffler K, Thieben F, Knopp T, Herrmann I K and Starsich F H 2022 *Nanoscale* **14** 7163–73
[26] Gavilán H, Avugadda S K, Fernández-Cabada T, Soni N, Cassani M, Mai B T, Chantrell R and Pellegrino T 2021 *Chem. Soc. Rev.* **50** 11614–67
[27] Chen W, Chen X, Yang M, Li S, Fan X, Zhang H and Xie H 2021 *ACS Appl. Mater. Interfaces* **13** 45315–24
[28] Barrera G, Allia P and Tiberto P 2020 *Nanoscale* **12** 6360–77
[29] Barrera G, Allia P and Tiberto P 2023 *Phys. Rev. Appl.* **19** 034029
[30] Elrefai A L, Enpuku K and Yoshida T 2021 *J. Appl. Phys.* **129** 1–11
[31] Socoliuc V, Peddis D, Petrenko V I, Avdeev M V, Susan-Resiga D, Szabó T, Turcu R, Tombácz E and Vékás L 2020 *Magnetochemistry* **6** 1–36
[32] Malhotra A, von Gladiss A, Behrends A, Friedrich T, Neumann A, Buzug T M and Lüdtke-Buzug K 2019 *Sci. Rep.* **9** 1–13
[33] Barrera G, Allia P and Tiberto P 2021 *J. Phys. D: Appl. Phys.* **54** 1–15
[34] Tulebayeva D Z, Kozlovskiy A, Korolkov I, Gorin Y G, Kazantsev A V, Abylgazina L, Shumskaya E E, Kaniukov E Y and Zdorovets M V 2018 *Mater. Res. Express* **5** 1–7
[35] Vasilakaki M, Ntallis N, Fiorani D, Peddis D and Trohidou K N 2022 *Nanoscale Adv.* **4** 4366–72
[36] Bertotti G 1998 *Hysteresis in Magnetism For Physicists, Materials Scientists and Engineers* (San Diego, CA: Academic)

[37] Barrera G, Allia P and Tiberto P 2021 *Nanoscale* **13** 4103–21
[38] Barrera G, Allia P and Tiberto P 2022 *ACS Appl. Nano Mater.* **5** 2699–714
[39] Allia P, Barrera G and Tiberto P 2020 *J. Magn. Magn. Mater.* **496** 1–14
[40] Barrera G, Allia P and Tiberto P 2022 *Phys. Rev. Appl.* **18** 1–18
[41] Schemberg J *et al* 2022 *ACS Appl. Mater. Interfaces* **14** 48011–28
[42] Ludwig F, Remmer H, Kuhlmann C, Wawrzik T, Arami H, Ferguson M and Krishnan K M 2015 *J. Magn. Magn. Mater.* **360** 169–73
[43] Ota S, Kitaguchi R, Takeda R, Yamada T and Takemura Y 2016 *Nanomaterials* **6** 1–11
[44] Draack S, Schilling M and Viereck T 2021 *Phys. Sci. Rev.* **8** 1–25
[45] Odenbach S (ed) 2022 *Magnetic Hybrid-Materials* (Berlin: Walter de Gruyter GmbH)
[46] Sasayama T, Yoshida T and Enpuku K 2017 *Jpn. J. Appl. Phys.* **56** 1–7
[47] Whitaker C 2017 *Master thesis* Engineering and Computer Science (available at: https://ir.library.oregonstate.edu/downloads/vd66w435j)
[48] Lenox P, Plummer L K, Paul P, Hutchison J E, Jander A and Dhagat P 2017 *IEEE Magn. Lett.* **9** 6500405
[49] Garaio E, Collantes J, Plazaola F, Garcia J and Castellanos-Rubio I 2014 *Meas. Sci. Technol.* **25** 115702
[50] Volchkov S O, Pasynkova A A, Derevyanko M S, Bukreev D A, Kozlov N V, Svalov A V and Semirov A V 2021 *Sensors* **21** 1–14
[51] Sciancalepore C, Bondioli F, Messori M, Barrera G, Tiberto P and Allia P 2015 *Polymer* **59** 278–89
[52] Barrera G, Coisson M, Celegato F, Raghuvanshi S, Mazaleyrat F, Kane S and Tiberto P 2018 *J. Magn. Magn. Mater.* **456** 372–80
[53] Barrera G, Serpe L, Celegato F, Cösson M, Martina K, Canaparo R and Tiberto P 2016 *Interface Focus* **6** 1–6
[54] Coïsson M, Barrera G, Celegato F, Martino L, Kane S, Raghuvanshi S, Vinai F and Tiberto P 2017 *Biochim. Biophys. Acta Gen. Subj.* **1861** 1545–58
[55] Grimnes S and Martinsen O G 2015 Instrumentation and measurement *Bioimpedence and Bioelectricity Basics* 3rd edn, ed S Grimnes and O G Martinsen (Amsterdam: Elsevier) ch 8, pp 255–328
[56] Enpuku K and Yoshida T 2020 Magnetic particle imaging *Bioimaging* ed S Ueno (Boca Raton, FL: CRC Press) ch 7, pp 155–83
[57] Jiles D and Atherton D 1984 *J. Appl. Phys.* **55** 2115–20
[58] Chikazumi S 1997 *Physics in Ferromagnetism* (Oxford: Oxford University Press)
[59] Cullity B D and Graham C D 2009 *Introduction to Magnetic Materials* (New York: Wiley)
[60] Nogués J and Schuller I K 1999 *J. Magn. Magn. Mater.* **192** 203–32
[61] Włodarczyk A, Gorgoń S, Radoń A and Bajdak-Rusinek K 2022 *Nanomaterials* **12** 1–23
[62] Duong H T K, Abdibastami A, Gloag L, Barrera L, Gooding J J and Tilley R D 2022 *Nanoscale* **14** 13890–914
[63] Beola L, Gutiérrez L, Grazú V and Asín L 2019 *A Roadmap to the Standardization of In Vivo Magnetic Hyperthermia* ed R Fratila and J M De La Fuente (Amsterdam: Elsevier) pp 317–37
[64] Rahmer J, Weizenecker J, Gleich B and Borgert J 2009 *BMC Med. Imaging* **9** 1–21
[65] Krycka K L, Rhyne J J, Oberdick S D, Abdelgawad A M, Borchers J A, Ijiri Y, Majetich S A and Lynn J W 2018 *New J. Phys.* **20** 1–9
[66] Saxena N, Dholia N, Akkireddy S, Singh A, Yadav U C S and Dube C L 2020 *Appl. Nanosci.* **10** 649–60
[67] Cowburn R, Koltsov D, Adeyeye A, Welland M and Tricker D 1999 *Phys. Rev. Lett.* **83** 1042–5
[68] Tiberto P, Barrera G, Celegato F, Conta G, Coïsson M, Vinai F and Albertini F 2015 *J. Appl. Phys.* **117** 1–4